HAL open science

Minimization of an energy error functional to solve a Cauchy problem arising in plasma physics: the reconstruction of the magnetic flux in the vacuum surrounding the plasma in a Tokamak

Blaise Faugeras, Amel Ben Abda, Jacques Blum, Cedric Boulbe

To cite this version:

Blaise Faugeras, Amel Ben Abda, Jacques Blum, Cedric Boulbe. Minimization of an energy error functional to solve a Cauchy problem arising in plasma physics: the reconstruction of the magnetic flux in the vacuum surrounding the plasma in a Tokamak. Revue Africaine de Recherche en Informatique et Mathématiques Appliquées, 2012, Volume 15, 2012, pp.37-60. 10.46298/arima.1957 . hal-00481257v3

HAL Id: hal-00481257

https://hal.science/hal-00481257v3

Submitted on 17 Nov 2013

HAL is a multi-disciplinary open access archive for the deposit and dissemination of scientific research documents, whether they are published or not. The documents may come from teaching and research institutions in France or abroad, or from public or private research centers.

L'archive ouverte pluridisciplinaire **HAL**, est destinée au dépôt et à la diffusion de documents scientifiques de niveau recherche, publiés ou non, émanant des établissements d'enseignement et de recherche français ou étrangers, des laboratoires publics ou privés.

Minimization of an energy error functional to solve a Cauchy problem arising in plasma physics: the reconstruction of the magnetic flux in the vacuum surrounding the plasma in a Tokamak

Blaise Faugeras*, Amel Ben Abda**,
Jacques Blum* and Cedric Boulbe*

* Laboratoire J.A. Dieudonné, UMR 7351, Université Nice Sophia Antipolis,
06108 Nice Cedex 02, France

** ENIT-LAMSIN, BP 37, 1002 Tunis, Tunisie

Email: Blaise.Faugeras@unice.fr

Abstract

A numerical method for the computation of the magnetic flux in the vacuum surrounding the plasma in a Tokamak is investigated. It is based on the formulation of a Cauchy problem which is solved through the minimization of an energy error functional. Several numerical experiments are conducted which show the efficiency of the method.

1 Introduction

In order to be able to control the plasma during a fusion experiment in a Tokamak it is mandatory to know its position in the vacuum vessel. This latter is deduced from the knowledge of the poloidal flux which itself relies on measurements of the magnetic field. In this paper we investigate a numerical method for the computation of the poloidal flux in the vacuum. Let us first briefly recall the equations modelizing the equilibrium of a plasma in a Tokamak [32].

Assuming an axisymmetric configuration one considers a 2D poloidal cross section of the vacuum vessel Ω_V in the (r, z) system of coordinates (Fig. 1). In this setting the poloidal flux $\psi(r, z)$ is related to the magnetic field through the relation $(B_r, B_z) = \frac{1}{r}(-\frac{\partial\psi}{\partial z}, \frac{\partial\psi}{\partial r})$ and, as there is no toroidal current density in the vacuum outside the plasma, satisfies the following equation

$$L\psi = 0 \text{ in } \Omega_X \tag{1}$$

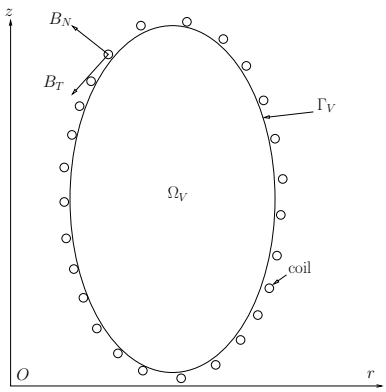

Figure 1: Cross section of the vacuum vessel: the domain Ω_V, its boundary Γ_V. Coils providing measurements of the components of the magnetic field tangent and normal to Γ_V are represented surrounding the vacuum vessel.

where L denotes the elliptic operator

$$L. = -[\frac{\partial}{\partial r}(\frac{1}{r}\frac{\partial .}{\partial r}) + \frac{\partial}{\partial z}(\frac{1}{r}\frac{\partial .}{\partial z})]$$

and

$$\Omega_X = \Omega_V - \bar{\Omega}_P$$

denotes the vacuum region surrounding the domain of the plasma Ω_P of boundary Γ_P (see Fig. 2). Inside the plasma Eq. (1) is not valid anymore and the poloidal flux satisfies the Grad-Shafranov equation [30, 16] which describes the equilibrium of a plasma confined by a magnetic field

$$L\psi = \mu_0 j(r, \psi) \text{ in } \Omega_P \tag{2}$$

where μ_0 is the magnetic permeability of the vacuum and $j(r, \psi)$ is the unknown toroidal current density function inside the plasma. Since the plasma boundary Γ_P is unknown the equilibrium of a plasma in a Tokamak is a free boundary problem described by a particular non-linearity of the model. The boundary is an iso-flux line determined either as being a magnetic separatrix (hyperbolic line with an X-point as on the left hand side of Fig. 2) or by the contact with a limiter (Fig. 2 right hand side). In other words the plasma boundary is determined from the equation $\psi(r, z) = \psi_P$, ψ_P being the value of the flux at the X-point or the value of the flux for the outermost flux line inside a limiter.

In order to compute an approximation of ψ in the vacuum and to find the plasma boundary without knowing the current density j in the plasma and thus without using the Grad-Shafranov equation (2) the strategy which is routinely used in operational codes mainly consists in choosing an a priori expansion method for ψ such as for example truncated Taylor and Fourier expansions

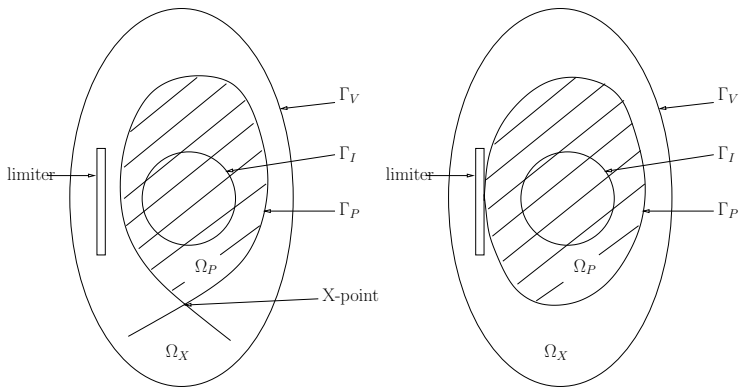

Figure 2: The plasma domain Ω_P and the vacuum region Ω_X. The plasma boundary is determined by an X-point configuration (left) or a limiter configuration (right). The fictitious contour Γ_I is represented inside the plasma.

for the code Apolo on the Tokamak ToreSupra [28] or piecewise polynomial expansions for the code Xloc on the Tokamak JET [26, 29]. The flux ψ can also be expanded in toroidal harmonics involving Legendre functions or expressed by using Green functions in the filament method ([23, 13], [9] and the references therein). In all cases the coefficients of the expansion are then computed through a fit to the measurements of the magnetic field. Indeed several magnetic probes and flux loops surround the boundary Γ_V of the vacuum vessel and measure the magnetic field and the flux (see Fig. 1). It should also be noted that very similar problems are studied in [18, 8, 14, 15]

In this paper we investigate a numerical method based on the resolution of a Cauchy problem introduced in ([6], Chapter 5) which we recall here below. The proposed approach uses the fact that after a preprocessing of these measurements (interpolation and possibly integration on a contour) one can have access to a complete set of Cauchy data, $f = \psi$ on Γ_V and $g = \dfrac{1}{r}\dfrac{\partial \psi}{\partial n}$ on Γ_V.

The poloidal flux satisfies

$$\begin{cases} L\psi = 0 \quad \text{in } \Omega_X \\ \psi = f \quad \text{on } \Gamma_V \\ \dfrac{1}{r}\dfrac{\partial \psi}{\partial n} = g \quad \text{on } \Gamma_V \\ \psi = \psi_P \quad \text{on } \Gamma_P \end{cases} \tag{3}$$

In this formulation the domain $\Omega_X = \Omega_X(\psi)$ is unknown since the free plasma boundary Γ_P as well as the flux ψ_P on the boundary are unknown. Moreover the problem is ill-posed in the sense of Hadamard [12] since there are two Cauchy conditions on the boundary Γ_V.

In order to compute the flux in the vacuum and to find the plasma boundary we are going to define a new problem as in [6] which is an approximation of the original one. Let us define a fictitious boundary Γ_I fixed inside the plasma (see Fig. 2). We are going to seek an approximation of the poloidal flux ψ satisfying $L\psi = 0$ in the domain contained between the fixed boundaries Γ_V and Γ_I. The problem becomes one formulated on a fixed domain Ω:

$$\begin{cases} L\psi = 0 \quad \text{in } \Omega \\ \\ \psi = f \quad \text{on } \Gamma_V \\ \\ \dfrac{1}{r}\dfrac{\partial \psi}{\partial n} = g \quad \text{on } \Gamma_V \end{cases} \tag{4}$$

Let us insist here on the fact that this problem is an approximation to the original one since in the domain between Γ_P and Γ_I, ψ should satisfy the Grad-Shafranov equation. The relevance of this approximating model is consolidated by the Cauchy-Kowalewska theorem [12]. For Γ_P smooth enough the function ψ can be extended in the sense of $L\psi = 0$ in a neighborhood of Γ_P inside the plasma. Hence the problem formulated on a fixed domain with a fictitious boundary Γ_I not "too far" from Γ_P is an approximation of the free boundary problem. As mentioned in [6] if Γ_I were identical with Γ_P then by the virtual shell principle [31] the quantity $w = \dfrac{1}{r}\dfrac{\partial \psi}{\partial n}|_{\Gamma_I}$ would represent the surface current density (up to a factor $\dfrac{1}{\mu_0}$) on Γ_P for which the magnetic field created outside the plasma by the current sheet is identical to the field created by the real current density spread throughout the plasma.

However no boundary condition is known on Γ_I. One way to deal with this second issue and to solve such a problem is to formulate it as an optimal control one. Only the Dirichlet condition on Γ_V is retained to solve the boundary value problem and a least square error functional measuring the distance between measured and computed normal derivative and depending on the unknown boundary condition on Γ_I is minimized. Due to the illposedness of the considered Cauchy problem a regularization term is needed to avoid erratic behaviour on the boundary where the data is missing. A drawback of this method developed in [6] is that Dirichlet and Neumann boundary conditions on Γ_V are not used in a symmetric way. One is used as a boundary condition for the partial differential equation, $L\psi = 0$, whereas the other is used in the functional to be minimized.

Freezing the domain to Ω by introducing the fictitious boundary Γ_I enables to remove the nonlinearity of the problem. The plasma boundary Γ_P can still be computed as an iso-flux line and thus is an output of our computations. We are going to compute a function ψ such that the Dirichlet boundary condition $u = \psi$ on Γ_I is such that the Cauchy conditions on Γ_V are satisfied as nearly as possible in the sense of the error functional defined in the next Section.

The originality of the approach proposed in this paper relies on the use of an error functional having a physical meaning: an energy error functional or

constitutive law error functional. Up to our knowledge this misfit functional has been introduced in [24] in the context of a posteriori estimator in the finite element method. In this context, the minimization of the constitutive law error functional allows to detect the reliability of the mesh without knowing the exact solution. Within the inverse problem community this functional has been introduced in [21, 22, 20] in the context of parameter identification. It has been widely exploited in the same context in [7]. It has also been used for Robin type boundary condition recovering [10] and in the context of geometrical flaws identification (see [4] and references therein). For lacking boundary data recovering (i.e. Cauchy problem resolution) in the context of Laplace operator, the energy error functional has been introduced in [2, 1]. A study of similar techniques can be found in [5, 3] and the analysis found in these papers uses elements taken from the domain decomposition framework [27].

The paper is organized as follows. In Section 2 we give the formulation of the problem we are interested in and provide an analysis of its well posedness. Section 3 describes the numerical method used. Several numerical experiments are conducted to validate it. The final experiment shows the reconstruction of the poloidal flux and the localization of the plasma boundary for an ITER configuration.

2 Formulation and analysis of the method

2.1 Problem formulation

As described in the Introduction the starting point is the free boundary problem (3). We first proceed as in [6] and in a first step consider the fictitious contour Γ_I fixed in the plasma and the fixed domain Ω contained between Γ_V and Γ_I. Problem (3) is approximated by the Cauchy problem (4). The boundaries Γ_V and Γ_I are assumed to be chosen smooth enough in order not to refrain any of the developments which follow in the paper.

In a second step the problem is separated into two different ones. In the first one we retain the Dirichlet boundary condition on Γ_V only, assume v is given on Γ_I and seek the solution ψ_D of the well-posed boundary value problem:

$$\begin{cases} L\psi_D = 0 & \text{in } \Omega \\ \psi_D = f & \text{on } \Gamma_V \\ \psi_D = v & \text{on } \Gamma_I \end{cases} \tag{5}$$

The solution ψ_D can be decomposed in a part linearly depending on v and a part depending on f only. We have the following decomposition:

$$\psi_D = \psi_D(v, f) = \psi_D(v, 0) + \psi_D(0, f) := \psi_D(v) + \tilde{\psi}_D(f) \tag{6}$$

where $\psi_D(v)$ and $\tilde{\psi}_D(f)$ satisfy:

$$\begin{cases} L\psi_D(v) = 0 \quad \text{in } \Omega \\ \psi_D(v) = 0 \quad \text{on } \Gamma_V \\ \psi_D(v) = v \quad \text{on } \Gamma_I \end{cases} \qquad \begin{cases} L\tilde{\psi}_D(f) = 0 \quad \text{in } \Omega \\ \tilde{\psi}_D(f) = f \quad \text{on } \Gamma_V \\ \tilde{\psi}_D(f) = 0 \quad \text{on } \Gamma_I \end{cases} \tag{7}$$

In the second problem we retain the Neumann boundary condition only and look for ψ_N satisfying the well-posed boundary value problem:

$$\begin{cases} L\psi_N = 0 \quad \text{in } \Omega \\ \dfrac{1}{r}\dfrac{\partial \psi_N}{\partial n} = g \quad \text{on } \Gamma_V \\ \psi_N = v \quad \text{on } \Gamma_I \end{cases} \tag{8}$$

in which ψ_N can be decomposed in a part linearly depending on v and a part depending on g only. We have the following decomposition:

$$\psi_N = \psi_N(v, g) = \psi_N(v, 0) + \psi_N(0, g) := \psi_N(v) + \tilde{\psi}_N(g) \tag{9}$$

where

$$\begin{cases} L\psi_N(v) = 0 \quad \text{in } \Omega \\ \dfrac{1}{r}\dfrac{\partial \psi_N(v)}{\partial n} = 0 \quad \text{on } \Gamma_V \\ \psi_N(v) = v \quad \text{on } \Gamma_I \end{cases} \qquad \begin{cases} L\tilde{\psi}_N(g) = 0 \quad \text{in } \Omega \\ \dfrac{1}{r}\dfrac{\partial \tilde{\psi}_N}{\partial n} = g \quad \text{on } \Gamma_V \\ \psi_N = 0 \quad \text{on } \Gamma_I \end{cases} \tag{10}$$

In order to solve problem (4), $f \in H^{1/2}(\Gamma_V)$ and $g \in H^{-1/2}(\Gamma_V)$ being given, we would like to find $u \in \mathcal{U} = H^{1/2}(\Gamma_I)$ such that $\psi = \psi_D(u, f) = \psi_N(u, g)$. To achieve this we are in fact going to seek u such that $J(u) = \inf_{v \in \mathcal{U}} J(v)$ where J is the error functional defined by

$$J(u) = \frac{1}{2}\int_\Omega \frac{1}{r}||\nabla\psi_D(u, f) - \nabla\psi_N(u, g)||^2 dx \tag{11}$$

measuring a misfit between the Dirichlet solution and the Neumann solution.

2.2 Analysis of the method

In order to minimize J one can compute its derivative and express the first order optimality condition. When doing so the two symmetric bilinear forms s_D and s_N as well as the linear form l defined below appear naturally and in a first step it is convenient to give a new expression of functional (11) using these forms.

Let $u, v \in H^{1/2}(\Gamma_I)$ and define

$$s_D(u, v) = \int_\Omega \frac{1}{r}\nabla\psi_D(u)\nabla\psi_D(v)dx \tag{12}$$

Applying Green's formula and noticing that $\psi_D(v) = v$ on Γ_I and $\psi_D(v) = 0$ on Γ_V we obtain

$$s_D(u,v) = \int_{\partial\Omega} \frac{1}{r}\partial_n\psi_D(u)\psi_D(v)d\sigma - \int_\Omega \nabla(\frac{1}{r}\nabla\psi_D(u))\psi_D(v)dx = \int_{\Gamma_I} \frac{1}{r}\partial_n\psi_D(u)vd\sigma \tag{13}$$

where the integrals on the boundary are to be understood as duality pairings. In Eq. (13) one can replace $\psi_D(v)$ by any extension $\mathcal{R}(v)$ in $H_0^1(\Omega,\Gamma_V) = \{\psi \in H^1(\Omega), \psi_{|\Gamma_V} = 0\}$ of $v \in H^{1/2}(\Gamma_I)$.
Hence s_D can be represented by

$$s_D(u,v) = \int_\Omega \frac{1}{r}\nabla\psi_D(u)\nabla\mathcal{R}(v)dx \tag{14}$$

Equivalently s_N is defined by

$$s_N(u,v) = \int_\Omega \frac{1}{r}\nabla\psi_N(u)\nabla\psi_N(v)dx \tag{15}$$

Since $\psi_N(v) = v$ on Γ_I and $\frac{1}{r}\partial_n\psi_N(u) = 0$ on Γ_V we have that

$$s_N(u,v) = \int_{\partial\Omega} \frac{1}{r}\partial_n\psi_N(u)\psi_N(v)d\sigma - \int_\Omega \nabla(\frac{1}{r}\nabla\psi_N(u))\psi_N(v)dx = \int_{\Gamma_I} \frac{1}{r}\partial_n\psi_N(u)vd\sigma \tag{16}$$

and s_N can also be represented by

$$s_N(u,v) = \int_\Omega \frac{1}{r}\nabla\psi_N(u)\nabla\mathcal{R}(v)dx \tag{17}$$

where $\mathcal{R}(v)$ is any extension in $H^1(\Omega)$ of $v \in H^{1/2}(\Gamma_I)$.

Let us now introduce

$$F(u,v) = \frac{1}{2}\int_\Omega \frac{1}{r}(\nabla\psi_D(u,f) - \nabla\psi_N(u,g))(\nabla\psi_D(v,f) - \nabla\psi_N(v,g))dx \tag{18}$$

such that $J(v) = F(v,v)$ and the linear form l defined by

$$l(v) = -\int_\Omega \frac{1}{r}(\nabla\tilde{\psi}_D(f) - \nabla\tilde{\psi}_N(g))\nabla\psi_D(v)dx \tag{19}$$

which can also be computed as

$$l(v) = -\int_\Omega \frac{1}{r}(\nabla\tilde{\psi}_D(f) - \nabla\tilde{\psi}_N(g))\nabla\mathcal{R}(v)dx \tag{20}$$

It can then be shown that

$$F(u,v) = \frac{1}{2}(s_D(u,v) - s_N(u,v) - l(u) - l(v)) + c \tag{21}$$

where the constant c is given by

$$c = \frac{1}{2}\int_\Omega \frac{1}{r}||\nabla\tilde{\psi}_D(f) - \nabla\tilde{\psi}_N(g)||^2 dx \tag{22}$$

Hence functional J can be rewritten as

$$J(v) = \frac{1}{2}(s_D(v,v) - s_N(v,v)) - l(v) + c \tag{23}$$

Following the analysis provided in [5] it can be proved that in the favorable case of compatible Cauchy data (f, g) the Cauchy problem admits a solution. There exists a unique $u \in \mathcal{U}$ such that $\psi_D(u, f) = \psi_N(u, g)$. The minimum of J is also uniquely reached at this point, $J(u) = 0$. This solution is given by the first order optimality condition which reads

$$(J'(u), v) = s_D(u,v) - s_N(u,v) - l(v) = 0 \quad \forall v \in \mathcal{U} \tag{24}$$

Equation (24) has an interpretation in terms of the normal derivative of ψ_D and ψ_N on the boundary. From Eqs. (13) and (16) and from

$$l(v) = -\int_\Omega \frac{1}{r}(\nabla\tilde{\psi}_D(f) - \nabla\tilde{\psi}_N(g))\nabla\psi_D(v)dx = -\int_{\Gamma_I} \frac{1}{r}(\partial_n\tilde{\psi}_D(f) - \partial_n\tilde{\psi}_N(g))v d\sigma \tag{25}$$

we deduce that the optimality condition can be rewritten as

$$\int_{\Gamma_I} [(\frac{1}{r}\partial_n\psi_D(u,f) - \frac{1}{r}\partial_n\psi_N(u,g))]v d\sigma = 0 \quad \forall v \in \mathcal{U} \tag{26}$$

which can be understood as the equality of the normal derivatives on Γ_I.

Hence the first optimality condition when minimizing J amounts to solve an interfacial equation

$$(S_D - S_N)(v) = \chi,$$

where S_D and S_N are the Dirichlet-to-Neumann operators associated to the bilinear forms and defined by:

$$\begin{array}{rcccl} S_D & : & H^{1/2}(\Gamma_I) & \longrightarrow & H^{-1/2}(\Gamma_I) \\ & & v & \longrightarrow & \frac{1}{r}\frac{\partial\psi_D(v)}{\partial n}. \end{array} \tag{27}$$

$$\begin{array}{rcccl} S_N & : & H^{1/2}(\Gamma_I) & \longrightarrow & H^{-1/2}(\Gamma_I) \\ & & v & \longrightarrow & \frac{1}{r}\frac{\partial\psi_N(v)}{\partial n}, \end{array} \tag{28}$$

and $\chi = -\frac{1}{r}\frac{\partial\tilde{\psi}_D}{\partial n} + \frac{1}{r}\frac{\partial\tilde{\psi}_N}{\partial n}$ on Γ_I.

Since S_D and S_N have the same eigenvectors and have asymptotically the same eigenvalues, the interfacial operator $S = S_D - S_N$ is almost singular [5]. This point together with the fact that the set of incompatible Cauchy data is

known to be dense in the set of compatible data (and thus numerical Cauchy data can hardly by compatible) make this inverse problem severely ill-posed.

Some regularization process has to be used. One way to regularize the problem is to directly deal with the resolution of the underlying quasi-singular linear system using for example a relaxed gradient method [2, 1]. In this paper we have chosen a regularization method of the Tikhonov type. It consists in shifting the spectrum of S by adding a term

$$(S_D - S_N) + \varepsilon S_D.$$

where ε is a small regularization parameter. This regularization method is quite natural since the ill-posedness of the inverse problem and the lack of stability in the identification of u by the minimization of J is strongly linked to the fact that J is not coercive (see [5] and below). We are thus going to minimize the regularized cost function:

$$J_\varepsilon(v) = J(v) + \varepsilon R_D(v)$$

with

$$R_D(v) = \frac{1}{2}\int_\Omega \frac{1}{r}||\nabla\psi_D(v)||^2 dx$$

This brings us to the framework described in [25]. We want to solve the following

$$\text{Problem } P_\varepsilon: \qquad \text{find } u_\varepsilon \in \mathcal{U} \text{ such that } J_\varepsilon(u_\varepsilon) = \inf_{v\in\mathcal{U}} J_\varepsilon(v)$$

and the following result holds.

Proposition 1 *1. Problem P_ε admits a unique solution $u_\varepsilon \in \mathcal{U}$ characterized by the first order optimality condition*

$$(J'_\varepsilon(u_\varepsilon), v) = \varepsilon s_D(u_\varepsilon, v) + s_D(u_\varepsilon, v) - s_N(u_\varepsilon, v) - l(v) = 0 \quad \forall v \in \mathcal{U} \quad (29)$$

2. For a fixed ε the solution is stable with respect to the data f and g. If f^1, $f^2 \in H^{1/2}(\Gamma_V)$ and g^1, $g^2 \in H^{-1/2}(\Gamma_V)$ it holds that

$$||u^1_\varepsilon - u^2_\varepsilon||_{H^{1/2}(\Gamma_I)} \leq \frac{C}{\varepsilon}(||f^1 - f^2||_{H^{1/2}(\Gamma_V)} + ||g^1 - g^2||_{H^{-1/2}(\Gamma_V)}) \quad (30)$$

3. If there exists $u \in \mathcal{U}$ such that $\psi_D(u, f) = \psi_N(u, g)$ then $u_\varepsilon \to u$ in $\mathcal{U}$ when $\varepsilon \to 0$.

Elements of the proof are given in Appendix.

3 Numerical method and experiments

3.1 Finite element discretization

The resolution of the boundary value problems (7) and (10) is based on a classical P^1 finite element method [11].

Let us consider the family of triangulation τ_h of Ω, and V_h the finite dimensional subspace of $H^1(\Omega)$ defined by

$$V_h = \{\psi_h \in H^1(\Omega), \psi_{h|T} \in P^1(T), \forall T \in \tau_h\}.$$

Let us also introduce the finite element space on Γ_I

$$D_h = \{v_h = \psi_h|_{\Gamma_I},\ \psi_h \in V_h\}.$$

Consider $(\phi_i)_{i=1,\dots N}$ a basis of V_h and assume that the first N_{Γ_I} mesh nodes (and basis functions) correspond to the ones situated on Γ_I. A function $\psi_h \in V_h$ is decomposed as $\psi_h = \sum_{i=1}^{N} a_i\phi_i$ and its trace on Γ_I as $v_h = \psi_h|_{\Gamma_I} = \sum_{i=1}^{N_{\Gamma_I}} a_i\phi_i|_{\Gamma_I}$.

Given boundary conditions v_h on Γ_I and f_h, g_h on Γ_V one can compute the approximations $\psi_{D,h}(v_h)$, $\psi_{N,h}(v_h)$, $\tilde{\psi}_{D,h}(f_h)$ and $\tilde{\psi}_{N,h}(g_h)$ with the finite element method.

In order to minimize the discrete regularized error functional, $J_{\varepsilon,h}(u_h)$ we have to solve the discrete optimality condition which reads

$$\varepsilon s_{D,h}(u_h, v_h) + s_{D,h}(u_h, v_h) - s_{N,h}(u_h, v_h) - l(v_h) = 0 \quad \forall v_h \in D_h \tag{31}$$

which is equivalent to look for the vector $\mathbf{u}$ solution to the linear system

$$\mathbf{S}\mathbf{u} = \mathbf{l} \tag{32}$$

where the $N_{\Gamma_I} \times N_{\Gamma_I}$ matrix $\mathbf{S}$ representing the bilinear form $s_h = \varepsilon s_{D,h} + s_{D,h} - s_{N,h}$ is defined by

$$\mathbf{S}_{ij} = s_h(\phi_i, \phi_j) \tag{33}$$

and $\mathbf{l}$ is the vector $(l_h(\phi_i))_{i=1,\dots N_{\Gamma_I}}$.

In order to lighten the computations the matrices are evaluated by

$$s_{D,h}(\phi_i, \phi_j) = \int_\Omega \frac{1}{r}\nabla\psi_{D,h}(\phi_i)\nabla\mathcal{R}(\phi_j)dx \tag{34}$$

and

$$s_{N,h}(\phi_i, \phi_j) = \int_\Omega \frac{1}{r}\nabla\psi_{N,h}(\phi_i)\nabla\mathcal{R}(\phi_j)dx \tag{35}$$

where $\mathcal{R}(\phi_j)$ is the trivial extension which coincides with ϕ_j on Γ_I and vanishes elsewhere.

In the same way the right hand side $\mathbf{l}$ is evaluated by

$$l_h(\phi_i) = -\int_\Omega \frac{1}{r}(\nabla\tilde{\psi}_{D,h}(f_h) - \nabla\tilde{\psi}_{N,h}(g_h))\nabla\mathcal{R}(\phi_i)dx \tag{36}$$

It should be noticed here that matrix **S** depends on the geometry of the problem only and not on the input Cauchy data. Therefore it can be computed once for all (as well as its LU decomposition for exemple if this is the method used to invert the system) and be used for the resolution of successive problems with varying input data as it is the case during a plasma shot in a Tokamak. Only the right hand side **l** has to be recomputed. This enables very fast computation times.

All the numerical results presented in the remaining part of this paper were obtained using the software FreeFem++ (http://www.freefem.org/ff++/). We are concerned with the geometry of ITER and the mesh used for the computations is shown on Fig. 3. It is composed of 1804 triangles and 977 nodes 150 of which are boundary nodes divided into 120 nodes on Γ_V and 30= N_{Γ_I} on Γ_I. The shape of Γ_I is chosen empirically.

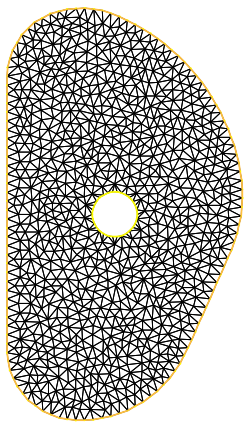

Figure 3: The mesh used for the ITER configuration in FreeFem++

3.2 Twin experiments

Numerical experiments with simulated input Cauchy data are conducted in order to validate the algorithm. Assume we are provided with a Neumann boundary condition function g on Γ_V. We generate the associated Dirichlet function f on Γ_V assuming a reference Dirichlet function u_{ref} is known on Γ_I. We thus solve the following boundary value problem:

$$\begin{cases} L\psi_{N,ref}(u_{ref}, g) = 0 \quad \text{in } \Omega \\ \\ \dfrac{1}{r}\partial_n \psi_{N,ref}(u_{ref}, g) = g \quad \text{on } \Gamma_V \\ \\ \psi_{N,ref}(u_{ref}, g) = u_{ref} \quad \text{on } \Gamma_I \end{cases} \tag{37}$$

noise level	error TC1	error TC2
0%	0.0131	0.0055
1%	0.0659	0.0170
5%	0.1526	0.0405

Table 1: Maximum relative error $\frac{|u_{opt} - u_{ref}|}{|u_{ref}|}$ for TC 1 and 2
.

and set $f = \psi_{N,ref}(u_{ref}, g)|_{\Gamma_V}$.

We have considered two test cases. In the first one (TC1)

$$u_{ref}(r, z) = 50 \sin(r)^2 + 50 \quad \text{on } \Gamma_I \tag{38}$$

and in the second one (TC2) u_{ref} is simply a constant

$$u_{ref}(r, z) = 40 \quad \text{on } \Gamma_I \tag{39}$$

The numerical experiments consist in minimizing the regularized error functional J_ε defined thanks to f and g. The obtained optimal solution u_{opt} and the associated ψ_{opt} are then compared to u_{ref} and ψ_{ref} which should ideally be recovered. Three cases are considered: the noise free case, a 1% noise on f and g and a 5% noise.

When the noise on f and g is small and the recovery of u is excellent there is very little difference between the Dirichlet solution $\psi_D(u_{opt}, f)$ and the Neumann solution $\psi_N(u_{opt}, g)$. However this is not the case any longer when the level of noise increases. The Dirichlet solution is much more sensitive to noise on f than the Neumann solution is sensitive to noise on g. Therefore the optimal solution is chosen to be $\psi_{opt} = \psi_N(u_{opt}, g)$.

The results are shown on Figs. 4 and 5 where the reference and recovered solutions are shown for the three levels of noise considered. The results are excellent for the noise free case in which the Dirichlet boundary condition u is almost perfecty recovered (Fig. 6). The differences between u_{opt} and u_{ref} increase with the level of noise (Fig. 6 and Tab. 1). As it is often the case in this type of inverse problems the most important errors on ψ_{opt} are localized close to the boundary Γ_I and vanishes as we move away from it (Fig. 7).

Tables 2 and 3 sumarize the evolution of the values of J, R_D and J_ε for the different noise level. First guess values ($u = 0$) are also provided for comparison. Please note that the regularization parameter was chosen differently from one experiment to another depending on the noise level. This was tuned by hand. In the next section we propose to use the L-curve method [19] to choose the value of ε.

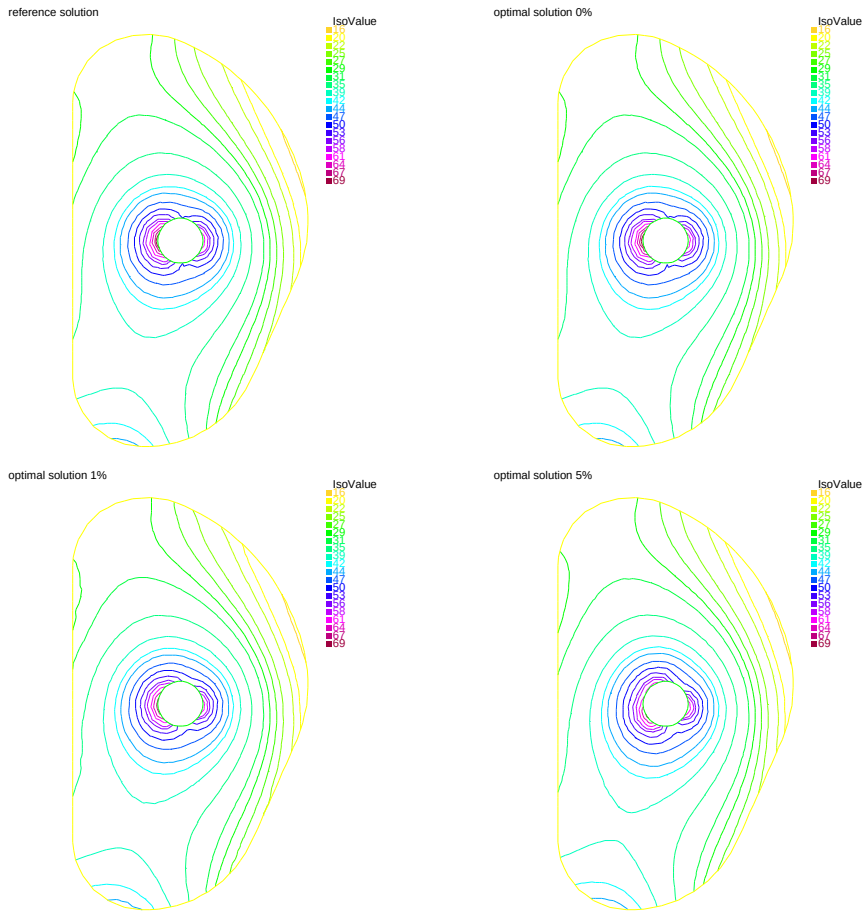

Figure 4: First test case (TC1), u_{ref} given by Eq. (38). Top left: reference solution $\psi_{N,ref}(u_{ref}, g)$. Top right: recovered solution with no noise on the data. Bottom left: recovered solution with a 1% noise on the data. Bottom right: recovered solution with a 5% noise.

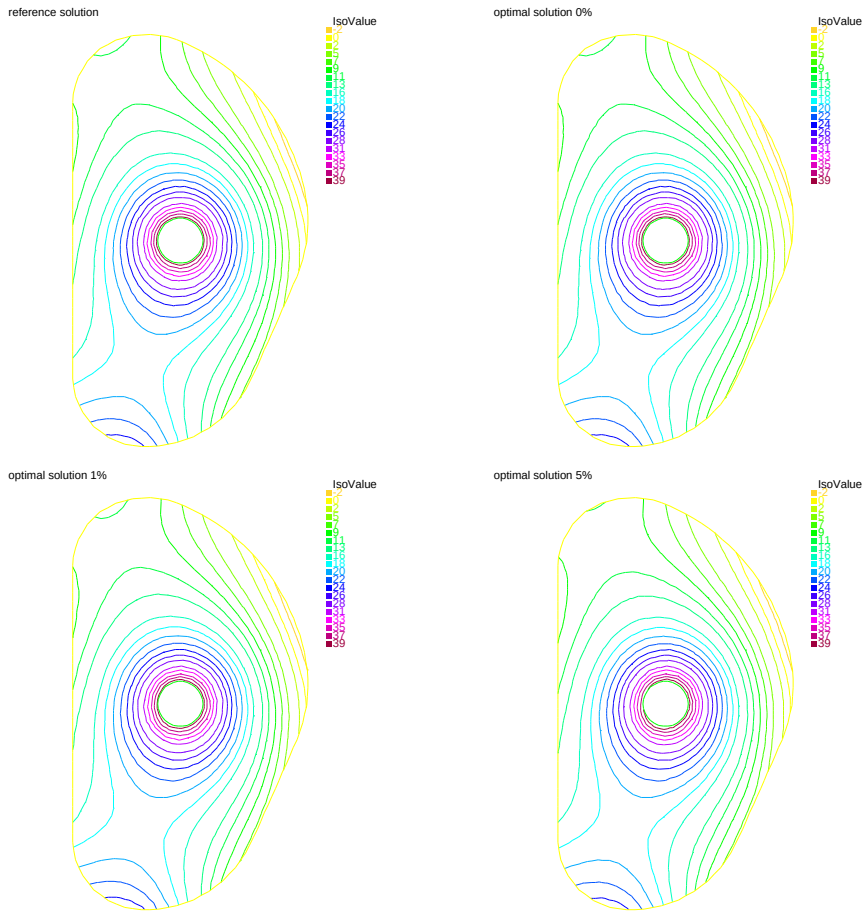

Figure 5: Second test case (TC2), u_{ref} given by Eq. (39). Top left: reference solution $\psi_{N,ref}(u_{ref}, g)$. Top right: recovered solution with no noise on the data. Bottom left: recovered solution with a 1% noise on the data. Bottom right: recovered solution with a 5% noise.

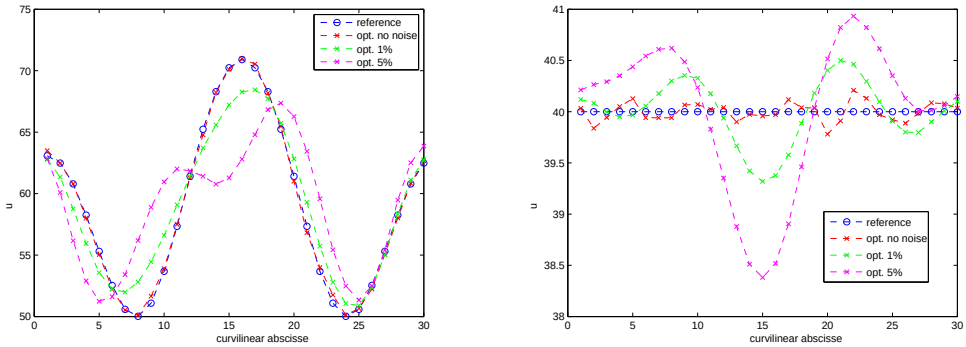

Figure 6: u_{ref} and the recovered u_{opt} for the 3 levels of noise on the data. Left: TC1. Right TC2.

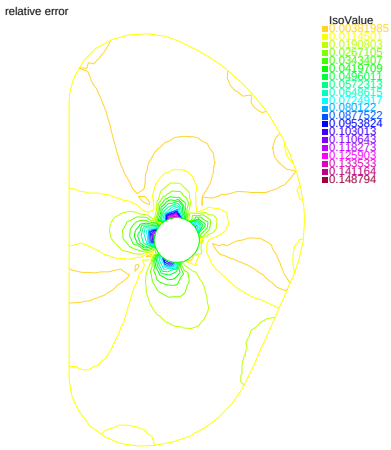

Figure 7: Relative error $|\psi_{opt} - \psi_{opt}|/|\psi_{ref}|$ for TC1 with 5% noise.

	J	R_D	J_ε	ε
$u = 0$ no noise	46.8643	0	46.8643	
u_{opt} no noise	0.0021	46.8722	0.0026	10^{-5}
u_{opt} 1% noise	1.8443	46.5553	1.8676	5×10^{-4}
u_{opt} 5% noise	9.2180	46.5575	9.2646	10^{-3}

Table 2: TC1 results. Values of the error functional, the regularization term, the total cost function and the chosen regularization parameter for the initial guess (row 1), the optimal solutions for different noise levels (row 2, 3 and 4).

	J	R_D	J_ε	ε
$u = 0$ no noise	30.7231	0	30.7231	
u_{opt} no noise	0.0003	30.7242	0.0006	10^{-5}
u_{opt} 1% noise	0.7300	30.7159	0.7607	10^{-3}
u_{opt} 5% noise	3.6516	30.6822	3.8050	5×10^{-3}

Table 3: TC2 results. Values of the error functional, the regularization term, the total cost function and the chosen regularization parameter for the initial guess (row 1), the optimal solutions for different noise levels (row 2, 3 and 4).

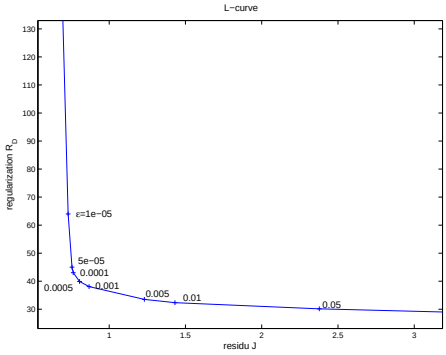

Figure 8: L-curve computed for the ITER case. The corner is located at $\varepsilon = 5 \times 10^{-4}$.

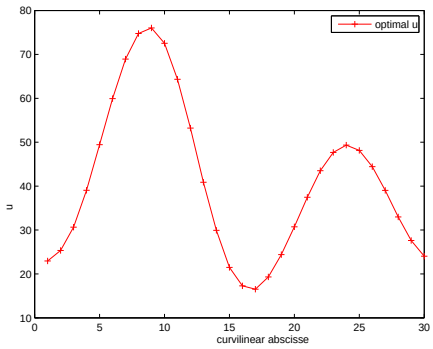

Figure 9: Optimal u_{opt} for the ITER case.

3.3 An ITER equilibrium

In this last numerical experiment we consider a 'real' ITER case. Measurements of the magnetic field are provided by the plasma equilibrium code CEDRES++ [17]. These mesurements are interpolated to provide f and g on Γ_V. The regularized error functional is then minimized to compute the optimal u_{opt}. The choice of the regularization parameter ε is made thanks to the computation of the L-curve shown on Fig. 8. It is a plot of $(J(u_{opt})(\varepsilon), R_D(u_{opt})(\varepsilon))$ as ε varies. The corner of the L-shaped curve provides a value of $\varepsilon = 5.10^{-4}$.

The computed u_{opt} is shown on Fig. 9 and numerical values are given in Tab. 4. The recovered poloidal flux ψ is shown on Fig. 10. The boundary of the plasma is found to be the isoflux $\psi = 16.3$ which shows an X-point configuration.

	J	R_D	J_ε	ε
$u = 0$	31.1026	0	31.1026	
u_{opt}	0.8053	39.9169	0.8253	5×10^{-4}

Table 4: ITER case results. Values of the error functional, the regularization term, the total cost function and the chosen regularization parameter for the initial guess (row 1) and the optimal solution (row 2)

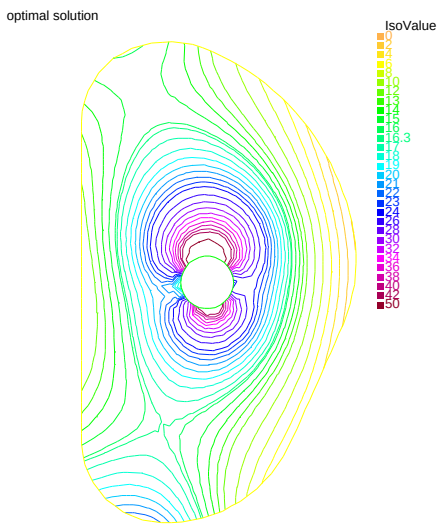

Figure 10: Optimal solution for the ITER case. The plasma is in an X-point configuration

4 Conclusion

We have presented a numerical method for the computation of the poloidal flux in the vacuum region surrounding the plasma in a Tokamak. The algorithm is based on the optimization of a regularized error functional. This computation enables in a second step the identification of the plasma boundary.

Numerical experiments have been conducted. They show that the method is precise and robust to noise on the Cauchy input data. It is fast since the optimization reduces to the resolution of a linear system of very reasonable dimension. Successive equilibrium reconstructions can be conducted very rapidly since the matrix of this linear system can be completely precomputed and only the right hand side has to be updated. The L-curve method proved to be efficient to specify the regularization parameter.

Appendix. Proof of Proposition 1

1. We need to prove the continuity and the coercivity of J_ε.
Continuity.
The maps $v \mapsto \psi_D(v)$ and $v \mapsto \psi_N(v)$ are continuous and linear from $H^{1/2}(\Gamma_I)$ to $H^1(\Omega)$. Moreover since $\tilde{\psi}_D(f)$ and $\tilde{\psi}_N(g)$ are in $H^1(\Omega)$ and $r_M \geq r \geq r_m > 0$ in Ω it is shown with Cauchy Schwarz that the bilinear forms s_D and s_N, the linear form l and thus J_ε are continuous on $H^{1/2}(\Gamma_I)$.

Coercivity.
The bilinear form s_D is coercive on $H^{1/2}(\Gamma_I)$. One obtains this from the fact that $\psi_D(v) \in H^1_0(\Omega, \Gamma_V)$ and the Poincaré inequality holds, and from the continuity of the application $\psi_D(v) \in H^1(\Omega) \to \psi_D(v)|_{\Gamma_I} = v \in H^{1/2}(\Gamma_I)$.

On the contrary, since for $\psi_N(v) \in H^1(\Omega)$ the seminorm does not bound the L^2 norm, the bilinear form s_N is not coercive and because of the minus sign in $s = s_D - s_N$ we need to prove that $s(v,v) \geq 0$ to obtain the coercivity of the bilinear part of functional J_ε. One can use the same type of argument as in [5] to de so.

Eventually it holds that

$$\frac{1}{2}s(v,v) + \frac{\varepsilon}{2}s_D(v,v) \geq C\varepsilon||v||^2_{H^{1/2}(\Gamma_I)}$$

Using the continuity and the coercivity of J_ε it results from [25] that problem P_ε admits a unique solution $u_\varepsilon \in \mathcal{U}$.

The solution u_ε is characterized by the first order optimality condition which is written as the following well-posed variational problem

$$(J'_\varepsilon(u_\varepsilon), v) = \varepsilon s_D(u_\varepsilon, v) + s_D(u_\varepsilon, v) - s_N(u_\varepsilon, v) - l(v) = 0 \quad \forall v \in \mathcal{U} \tag{40}$$

which as in Eq. (26) can be understood as an equality on Γ_I.

2. The stability result is deduced from the optimality condition (40).

Let u^1_ε (resp. u^2_ε) be the solution associated to (f^1, g^1) (resp. (f^2, g^2)). Substracting the two optimality conditions, choosing $v = u^1_\varepsilon - u^2_\varepsilon$ and using the coercivity leads to

$$C\varepsilon||u^1_\varepsilon - u^2_\varepsilon||^2_{H^{1/2}(\Gamma_I)} \leq |(l_1 - l_2)(u^1_\varepsilon - u^2_\varepsilon)|$$

The map $f \mapsto \tilde{\psi}_D(f)$ is linear and continuous from $H^{1/2}(\Gamma_V)$ to $H^1(\Omega)$, and so is the map $g \mapsto \tilde{\psi}_N(g)$ from $H^{-1/2}(\Gamma_V)$ to $H^1(\Omega)$. Using these facts and Cauchy Schwarz it follows that

$$||u^1_\varepsilon - u^2_\varepsilon||_{H^{1/2}(\Gamma_I)} \leq \frac{C'}{r_m C}\frac{1}{\varepsilon}(||f^1 - f^2||_{H^{1/2}(\Gamma_V)} + ||g^1 - g^2||_{H^{-1/2}(\Gamma_V)})$$

3. For this point the proof of Proposition 3.2 in [3] can be adpated. A sketch of the proof is as follows. Let us suppose that there exists $u \in \mathcal{U}$ such

that $\psi_D(u,f) = \psi_N(u,g)$. A key point is to show that $s_D(u_\varepsilon, u_\varepsilon) \to s_D(u,u)$ when $\varepsilon \to 0$. Then in a second step using the optimality conditions for u and u_ε it is shown that

$$s_D(u_\varepsilon - u, u_\varepsilon - u) \leq s_D(u,u) - s_D(u_\varepsilon, u_\varepsilon)$$

which gives the result thanks to the coercivity of s_D in $H^{1/2}(\Gamma_I)$.

References

[1] S. Andrieux, T.N. Baranger, and A. Ben Abda. Solving cauchy problems by minimizing an energy-like functional. *Inverse Problems*, 22:115–133, 2006.

[2] S. Andrieux, A. Ben Abda, and T.N. Baranger. Data completion via an energy error functional. *C.R. Mecanique*, 333:171–177, 2005.

[3] M. Azaiez, F. Ben Belgacem, and H. El Fekih. On Cauchy's problem: II. Completion, regularization and approximation. *Inverse Problems*, 22:1307–1336, 2006.

[4] A Ben Abda, M. Hassine, M. Jaoua, and M. Masmoudi. Topological sensitivity analysis for the location of small cavities in stokes flows. *SIAM J. Cont. Opt.*, 2009.

[5] F. Ben Belgacem and H. El Fekih. On Cauchy's problem: I. A variational Steklov-Poincaré theory. *Inverse Problems*, 21:1915–1936, 2005.

[6] J. Blum. *Numerical Simulation and Optimal Control in Plasma Physics with Applications to Tokamaks.* Series in Modern Applied Mathematics. Wiley Gauthier-Villars, Paris, 1989.

[7] M. Bonnet and A. Constantinescu. Inverse problems in elasticity. *Inverse Problems*, 21(2), 2005.

[8] L. Bourgeois and J. Dardé. A quasi-reversibility approach to solve the inverse obstacle problem. *Inverse Problems and Imaging*, 4/3:351–377, 2010.

[9] B.J. Braams. The interpretation of tokamak magnetic diagnostics. *Nuc. Fus.*, 33(7):715–748, 1991.

[10] S. Chaabane and M. Jaoua. Identification of robin coefficients by means of boundary measurements. *Inverse Problems*, 15(6):1425, 1999.

[11] P.G. Ciarlet. *The Finite Element Method For Elliptic Problems.* North-Holland, 1980.

[12] R. Courant and D. Hilbert. *Methods of Mathematical Physics*, volume 1-2. Interscience, 1962.

[13] W. Feneberg, K. Lackner, and P. Martin. Fast control of the plasma surface. *Computer Physics Communications*, 31(2):143–148, 1984.

[14] Y. Fischer. *Approximation dans des classes de fonctions analytiques généralisées et résolution de problèmes inverses pour les tokamaks.* Phd thesis, Université de Nice Sophia Antipolis, France, 2011.

[15] Y. Fischer, B. Marteau, and Y. Privat. Some inverse problems around the tokamak tore supra. *Comm. Pure and Applied Analysis*, to appear.

[16] H. Grad and H. Rubin. Hydromagnetic equilibria and force-free fields. In *2nd U.N. Conference on the Peaceful uses of Atomic Energy*, volume 31, pages 190–197, Geneva, 1958.

[17] V. Grandgirard. *Modélisation de l'équilibre d'un plasma de tokamak - Tokamak plasma equilibrium modelling.* Phd thesis, Université de Besançon, France, 1999.

[18] H. Haddar and R. Kress. Conformal mappings and inverse boundary value problem. *Inverse Problems*, 21:935–953, 2005.

[19] C. Hansen. *Rank-Deficient and Discrete Ill-Posed Problems: Numerical Aspects of Linear Inversion.* SIAM, Philadelphia, 1998.

[20] R.V. Kohn and A. McKenney. Numerical implementation of a variational method for electrical impedance tomography. *Inverse Problems*, 6(3):389, 1990.

[21] R.V. Kohn and M.S. Vogelius. Determining conductivity by boundary measurements: II. Interior results. *Commun. Pure Appl. Math.*, 31:643–667, 1985.

[22] R.V. Kohn and M.S. Vogelius. Relaxation of a variational method for impedance computed tomography. *Commun. Pure Appl. Math.*, 11:745–777, 1987.

[23] K. Lackner. Computation of ideal MHD equilibria. *Computer Physics Communications*, 12:33–44, 1976.

[24] P. Ladeveze and D. Leguillon. Error estimate procedure in the finite element method and applications. *SIAM J. Num. Anal.*, 20(3):485–509, 1983.

[25] J.L. Lions. *Contrôle optimal de systèmes gouvernés par des équations aux dérivées partielles (Optimal control of systems governed by partial differential equations).* Dunod, Paris, 1968.

[26] D.P. O'Brien, J.J Ellis, and J. Lingertat. Local expansion method for fast plasma boundary identification in JET. *Nuc. Fus.*, 33(3):467–474, 1993.

[27] A. Quarteroni and V Alberto. *Domain Decomposition Methods for Partial Differential Equations.* Oxford University Press, 1999.

[28] F. Saint-Laurent and G. Martin. Real time determination and control of the plasma localisation and internal inductance in Tore Supra. *Fusion Engineering and Design*, 56-57:761–765, 2001.

[29] F. Sartori, A. Cenedese, and F. Milani. JET real-time object-oriented code for plasma boundary reconstruction. *Fus. Engin. Des.*, 66-68:735–739, 2003.

[30] V.D. Shafranov. On magnetohydrodynamical equilibrium configurations. *Soviet Physics JETP*, 6(3):1013, 1958.

[31] V.D. Shafranov and L.E. Zakharov. Use of the virtual-casing principle in calculating the containing magnetic field in toroidal plasma systems. *Nuc. Fus.*, 12:599–601, 1972.

[32] J. Wesson. *Tokamaks*, volume 118 of *International Series of Monographs on Physics*. Oxford University Press Inc., New York, Third Edition, 2004.